

IMPULSIVE FREE-SURFACE FLOW DUE TO A STEADY LINE SOURCE AT THE BOTTOM OF A UNIFORM FLUID LAYER

Maurizio Landrini

INSEAN, The Italian Ship Model Basin
Via di Vallerano 139, 00128 Roma. Italy

Peder A. Tyvand

Department of Agricultural Engineering
Agricultural University of Norway
Box 5065, N-1432 Aas Norway

Introduction

The classical Cauchy-Poisson problem assumes the initial surface elevation and surface velocity to be given at time zero. The resulting free-surface flow is calculated according to linear theory. The present work is concerned with the Cauchy-Poisson problem for constant depth [1, 2]. Specifically, we consider the flow due to normal velocity at the bottom instead of initial surface disturbances.

We will investigate the basic case of a steady source (or sink) located at the bottom by analytical and numerical means. Such singularities, turned on impulsively at time zero, generate interesting classes of nonlinear wave systems governed uniquely by a Froude number. A source will generate a bore, from undular type to breaking dependent on the Froude number. The steady sink may give rise to dip instability, where the free surface collapses into the sink.

Problem formulation

We consider an inviscid, incompressible fluid layer of infinite width and constant depth h^* . The motion is two-dimensional and starts from rest with uniform zero wave elevation. According to Kelvin's theorem the motion is irrotational. A steady source (sink) is turned on impulsively at time $t^* = 0$. It has volume flux Q^* per length unit perpendicular to the plane of motion. The singularity is located at the bottom point $(x, y) = (0, -h^*)$. The relevant dimensionless parameter is the Froude number of the source:

$$F = Q^* / \sqrt{g^* h^{*3}} \quad (1)$$

As unit of dimensionless length we take h^* . Our primary units of dimensionless time and velocity are Q^*/h^* and h^{*2}/Q^* , respectively. This are relevant for the small-time behaviour of the nonlinear free-surface flow. For the large-time evolution, gravity plays an dominant role and we have to resort to the alternative gravitational units of dimensionless time and velocity: $\sqrt{h^*/g^*}$ and $\sqrt{g^*/h^*}$, respectively.

The velocity potential Φ satisfies Laplace's equation, with (fully nonlinear) boundary conditions on the free surface:

$$\frac{\partial \eta}{\partial t} + \nabla \Phi \cdot \nabla \eta = \frac{\partial \Phi}{\partial y} \quad \frac{\partial \Phi}{\partial t} + \frac{1}{2} |\nabla \Phi|^2 + \frac{1}{F^2} \eta = 0 \quad \text{on } y = \eta(x, t) \quad (2)$$

and a no-penetration condition at the bottom.

Analytical and numerical results

For small time t we can solve the nonlinear problem asymptotically by a small-time expansion:

$$(\Phi, \eta) = H(t)[(\Phi_0, 0) + t(\Phi_1, \eta_1) + t^2(\Phi_2, \eta_2) + \dots] \quad -\infty < t < \infty \quad (3)$$

where $H(t)$ is the Heaviside unit step function. To each order, Laplace's equation is valid in the undisturbed fluid domain:

$$\nabla^2 \Phi_n = 0 \quad -1 < y < 0 \quad (n = 0, 1, 2, \dots) \quad (4)$$

The boundary conditions are:

$$\Phi_0 = 0 \quad \Phi_1 = -\frac{1}{2} \eta_1^2 \quad \Phi_2 = -\eta_1(2\eta_2 + \frac{1}{2F^2}) \quad (5a)$$

$$\eta_1 = \frac{\partial \Phi_0}{\partial y} \quad \eta_2 = \frac{1}{2} \frac{\partial \Phi_1}{\partial y} \quad \eta_3 = \frac{1}{3} \frac{\partial \Phi_2}{\partial y} + \frac{1}{6} \eta_1^2 \frac{d^2 \eta_1}{dx^2} + \frac{1}{3} \eta_1 \left| \frac{d\eta_1}{dx} \right|^2 \quad (5b)$$

on the free surface, while on the bottom holds:

$$\frac{\partial \Phi_0}{\partial y} = \delta(x) \quad y = -1, \quad t > 0 \quad (6)$$

only for the zeroth order potential. Upon introducing an (inessential) spatial artificial periodicity (with fundamental wavenumber k) and after some manipulations, the first-order elevation reads:

$$\eta_1 = \frac{1}{2} \operatorname{sech} \pi \frac{x}{2} \simeq \frac{2k}{\pi} \sum_{n \text{ odd}} \operatorname{sech} k_n \cos k_n x \quad (7)$$

where both the exact and the approximate solutions are given, and $k_n = nk$. The second- and third-order solutions can be obtained only in the form of multiple series expansions:

$$\eta_2 = -\frac{1}{2} \left(\frac{k}{\pi}\right)^2 \sum_n \sum_{\text{odd } m} \sum_{\text{odd}} \text{sech } k_n \text{sech } k_m [k_{n-m} \tanh k_{n-m} \cos(k_{n-m}x) + k_{n+m} \tanh k_{n+m} \cos(k_{n+m}x)] - \sigma \frac{1}{4} \text{sech}\left(\frac{\pi}{2}x\right) \quad (8)$$

and

$$\begin{aligned} \eta_3 = & \frac{1}{3} \left(\frac{k}{\pi}\right)^3 \sum_n \sum_{\text{odd } m} \sum_{\text{odd } q} \sum_{\text{odd}} \text{sech } k_n \text{sech } k_m \text{sech } k_q \times \\ & \{ k_{n-m} \tanh k_{n-m} [k_{n-m-q} \tanh k_{n-m-q} \cos(k_{n-m-q}x) + k_{n-m+q} \tanh k_{n-m+q} \cos(k_{n-m+q}x)] \\ & + k_{n+m} \tanh k_{n+m} [k_{n+m-q} \tanh k_{n+m-q} \cos(k_{n+m-q}x) + k_{n+m+q} \tanh k_{n+m+q} \cos(k_{n+m+q}x)] \} \\ & + \frac{2}{3} \sigma \left(\frac{k}{\pi}\right)^2 \sum_n \sum_{\text{odd } m} \sum_{\text{odd}} \text{sech } k_n \text{sech } k_m [k_{n-m} \tanh k_{n-m} \cos(k_{n-m}x) + k_{n+m} \tanh k_{n+m} \cos(k_{n+m}x)] \\ & - \frac{1}{3F^2} \frac{k}{\pi} \sum_n \sum_{\text{odd}} k_n \text{sech } k_n \tanh k_n \cos k_n x + \frac{\pi^2}{384} \text{sech}^5\left(\frac{\pi}{2}x\right) [3 \cosh(\pi x) - 5] + \frac{\sigma^2}{12} \text{sech}\left(\frac{\pi}{2}x\right) \end{aligned} \quad (9)$$

respectively. The solution for a sink at the bottom can be obtained simply by changing the sign of η_1 and η_3 .

Figure 1 shows the comparison between the small time expansion and the numerical solution of the exact problem obtained by a boundary integral equation method. Apparently, significant differences between the two solutions appear for $t > 1$. As it can be expected, for a source weak enough, the flow develops in the

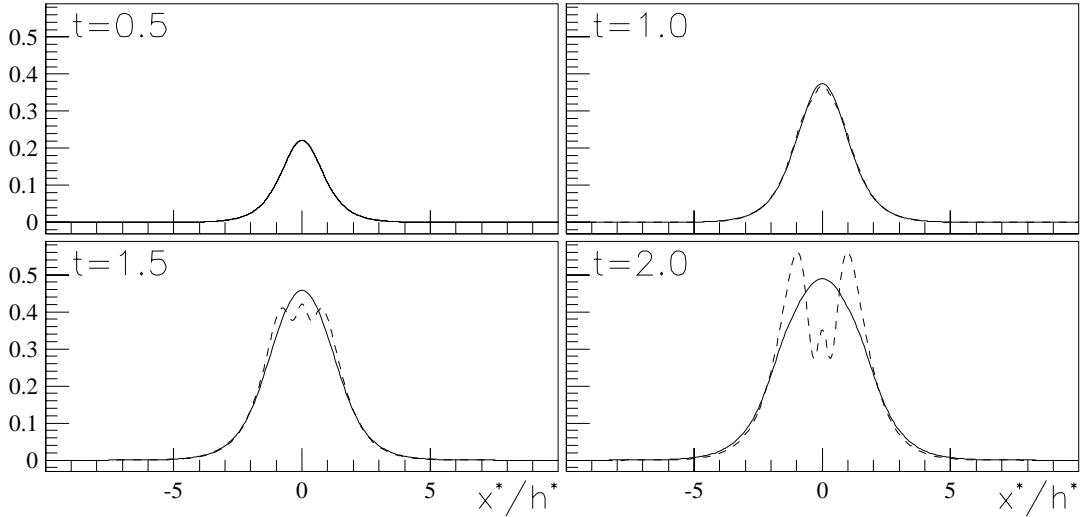


Figure 1: Comparison between the small time expansion solution (dashed lines) and the numerical computations (solid-lines) for $F = 1.0$. Non-dimensional time $t = t^*Q^*/h^{*2}$.

form of an undular bore (cfr. fig. 2) which cannot be followed by the present small time expansion solution. Therefore, for larger time we find alternative analytical solutions. To the purpose, we switch from the units of dimensionless time and velocity above introduced to the gravitational units. By integrating up in time the asymptotic solution given in [2], we get an asymptotic solution for the (linearized) surface elevation

$$\eta = \frac{1}{2} F \int_0^t (2/(t-\tau))^{1/3} \text{Ai}[(2/(t-\tau))^{1/3}(|x| + \tau - t)] d\tau \quad (10)$$

in terms of the Airy function. In this equation we assume that the wave front has propagated many length units. The comparison between the asymptotic formula and the fully nonlinear solution is given in figure 2, where also the linear solution is plotted. Apparently, although the phenomenon is qualitatively well captured, the fully nonlinear bore-front is steeper and propagates faster. These differences are magnified by further increasing the source strength.

The undular bore leaves behind it an almost flat free surface with height $\eta_b = F/2$ according to a linear theory. As it can be seen in the same figure, the fully nonlinear numerical solution predicts a smaller η_b . We now give an analytical estimate of the free surface height η_b past the bore. The analysis follows from a simple mass conservation argument, where we apply the amplitude dispersion $c = 1 + 3\eta_b/2$ given by the

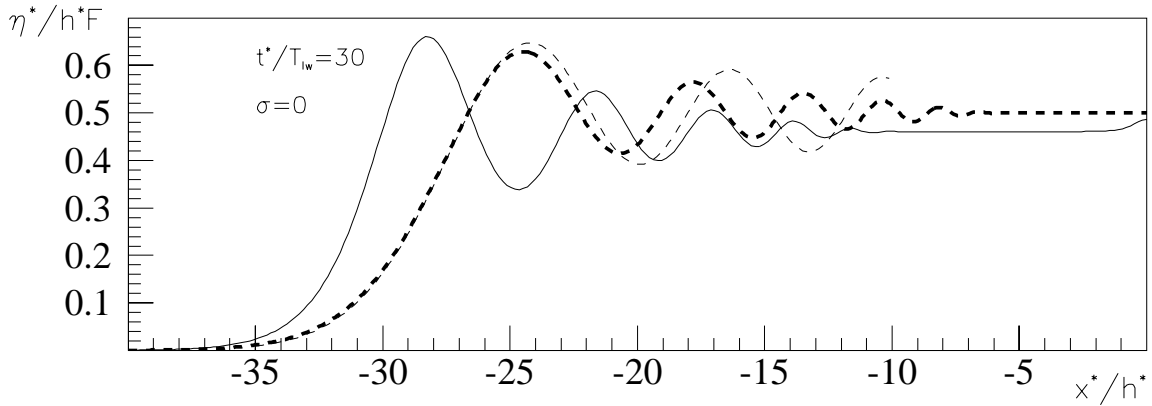


Figure 2: Undular bore due to a steady sink ($F = 0.25$). Bore-fronts as predicted by the asymptotic formula (10) (thin dashed line), linear (thick dashed line) and fully nonlinear computations (solid line).

Korteweg-deVries equation. We consider a trapezoid model where the midpoint of the bore front has half the amplitude dispersion of the bulk of the bore. This gives the analytical formula

$$\eta_b = \frac{2}{3} \left(\sqrt{1 + \frac{3}{2}F} - 1 \right) \quad (11)$$

for the surface elevation in the bulk of the bore, which is in a remarkable good agreement with our numerical computations (for non-breaking cases):

	$F = 0.5$	$F = 0.25$	$F = 0.125$	$F = 0.0625$
η_b from eq. (11)	0.4305	0.4603	0.4785	0.4888
η_b from num. sim.	0.4318	0.4608	0.4786	0.4888

In numerical computations, increasing the source strength, the front of the bore-front steepens and eventually a breaker develops. In particular, for larger F the breaking event appears sooner and a larger plunger is featured (cfr. fig. 3). Our results rely on a fully nonlinear model and improve the earlier shallow-water computations in [3]. A further step could be coupling with the steady breaker solution in [4].

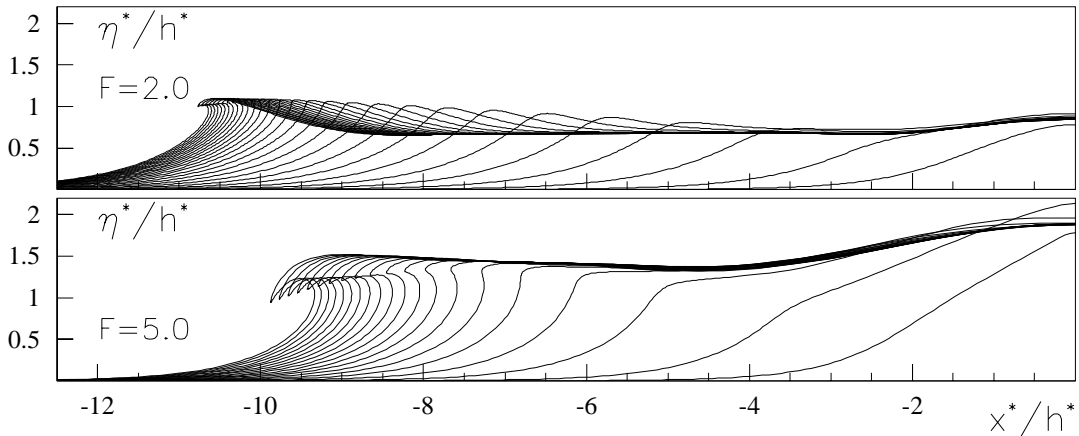


Figure 3: Evolution toward breaking of the bore due to a source, $F = 2$ and 5.

The asymptotic formula (10) equally applies to the case of a submerged sink. Unlike the previous case, nonlinearities delay the propagation of the front which, now, leaves behind it a depression (see fig. 4). As it can be expected, the stronger the sink is, the deeper the depression will be. More peculiar, the free surface is now characterized by a number of high frequency oscillations.

For a stronger suction of the sink, the free surface collapses into the bottom singularity [5, 6, 7]. According to the small-time expansion, the critical Froude number for the early tendency towards dip instability is $F_c = 4/\pi$. For this value we have $\eta_3(0) = 0$ and the nonlinear suction into the sink is exactly balanced by the gravitational rebound to the leading order. Xue & Yue (1998), for the deep water axisymmetric case, evidenced that the dip formation is a strongly nonlinear phenomenon which cannot be decided by small-time asymptotics. Actually, we numerically found an intermediate range of $-F$ (cfr. fig. 5) for which a hump emerges from the nascent dip and gives rise to a couple of symmetric plunging breakers. For increasing $-F$,

the horizontal separation of the breaking waves decreases. For stronger suction, the hump reduces to narrow bulge of fluid and, eventually, to a jet emitted from the collapsing dip. Only for a stronger sink, the fluid collapses continuously toward the singularity.

We have studied nonlinear free-surface flows generated by an impulsive bottom source or sink. Compared with earlier work on submerged singularities in deep water, we observed a much stronger tendency towards wave breaking, due to the weaker dispersion of a wave packet propagating on finite depth. Details of the breaking vary with the Froude number of the source/sink. Wave breaking appears also for sinks somewhat too weak for dip instability: this terminates our computations and thereby disturbs our search for a clear dip instability criterion. For the bottom source, another challenge remains for future work: Is there a steady bore solution of the fully nonlinear free-surface problem?

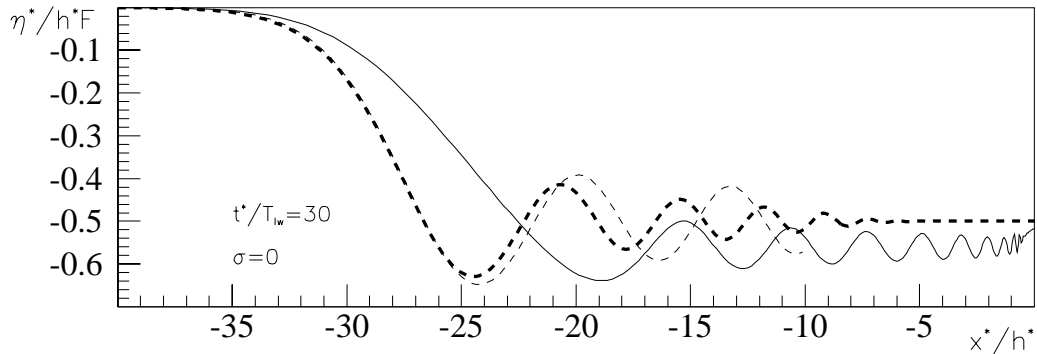


Figure 4: Free surface due to a constant sink ($F = -0.25$). Comparison of asymptotic prediction (thin dashed line), linear (thick dashed line) and nonlinear computations (solid line).

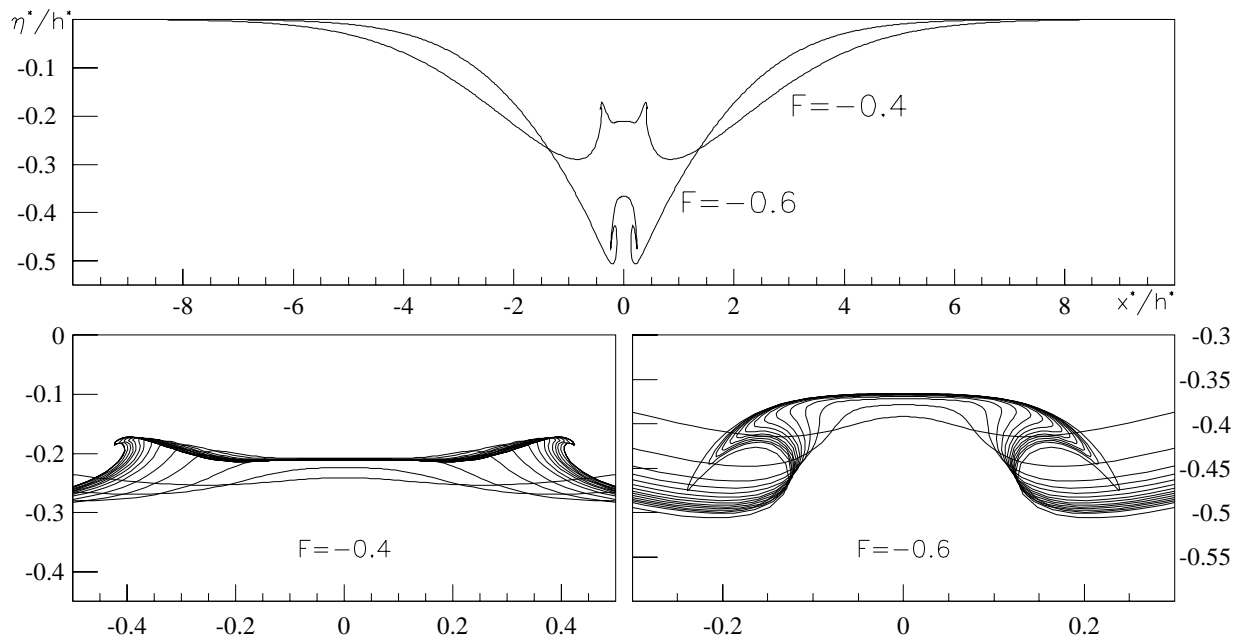


Figure 5: Free surface due to a constant sink. Top: free surface for $F = -0.4$ ($t = 4.42$) and $F = -0.6$ ($t = 2.88$). Bottom: enlarged view in natural scale of the free surface around the sink.

The research activity of M.L. is supported by the Italian *Ministero dei Trasporti e della Navigazione* through INSEAN Research Project 2000-2002.

1. Wehausen, J.V. & Laitone, E. V. 1960 Handbuch der Physik, ed. W. Flugge, vol. 9, pp. 446-778, Springer-Verlag.
2. Whitham, G.B. 1974 Linear and Nonlinear Waves. J. Wiley, New York.
3. Peregrine, D.H. 1966 Calculations of the development of an undular bore, J. Fluid Mech. 25, 321-330.
4. Cointe, R. & Tulin, M. P. 1994 A theory of steady breakers. J. Fluid Mech., **276**.
5. Tyvand, P.A. 1992 Unsteady free-surface flow due to a line source. Phys. Fluids A4, 671-676.
6. Xue, M. & Yue, D.K.P. 1998 Nonlinear free-surface flow due to an impulsively-started submerged point sink. J. Fluid Mech. 364, 325-347.
7. Miloh, T. & Tyvand, P.A. 1993 Non-linear transient free-surface flow and dip formation due to a point sink. Phys. Fluids A5, 1368-1375.